

SOME ASPECTS OF FUSION REACTIONS IN THE TANDEM ENERGY REGION

Christian NGÔ

FR 33-300!

DPH-W/MF, CEN Saclay, Bât. 34, 91191 Gif-sur-Yvette Cedex, France

Abstract

We review the following aspects of fusion reactions in the tandem energy region : the experimental definition of the fusion, the experimental techniques to measure fusion cross sections, the analysis of the data in terms of critical angular momentum, the static and dynamical interpretations of the fusion process.

Tandem accelerators are very useful tools for investigating the fusion process. In the energy range provided by these accelerators the fusion cross section is a large part of the total reaction cross section. Up to now an overall understanding of the fusion process has been reached but many questions still remain open. Therefore many careful and systematic investigations are needed for a complete understanding of this phenomenon.

It is of great interest, for many purposes, to realize the fusion of two heavy ions. For instance in order to investigate highly excited nuclei, to learn about high spin states, to synthesise exotic nuclei etc... Furthermore the fusion process is also very fascinating in itself because it is the most dissipative mechanism investigated so far in heavy ion collisions : all the nucleons of the system are involved, all the initial kinetic energy in the relative motion of the incident ions is transformed into excitation energy of the fused system, all the orbital angular momentum is also lost creating in this way highly rotating compound nuclei. Therefore, it is crucial to know under which conditions two heavy ions can fuse together.

1. Experimental definition of the fusion cross section

When two heavy ions fuse together we usually form a compound nucleus, or something close to it, with some excitation energy and angular momentum. Consequently it will deexcite by emitting light particles and γ rays leading to what is called residual nucleus, and, if the fission barrier is small or reduced sufficiently by angular momentum, it will fission.

The fusion cross section, σ_F , is defined as the sum of two terms : the evaporation residue cross section, σ_{ER} , which corresponds to nuclei with a mass close to the one of the compound nucleus, and the fission cross section, σ_f , which corresponds to products which have a symmetric mass distribution around a mean value which is about half the compound nucleus mass

$$\sigma_F = \sigma_{ER} + \sigma_f \quad (1)$$

When light compound nuclei are formed, the evaporation residue cross section is a large part of the fusion cross section. It is the contrary for heavy compound nuclei where the fission cross section is almost identical to σ_F . When very heavy projectiles are involved, the fusion cross section goes to zero. This happens more precisely when the product $Z_1 Z_2$ of the atomic numbers of the projectile and target nuclei is larger than about 2500-3000. On the other hand, at bombarding energies larger than about 10 MeV/A the fusion between the two incident nuclei is no longer complete in the sense that all the nucleons merge into a single excited system. Fast particles, p, n, α , ... can be emitted at the very beginning of the reaction and the two remaining fragments can subsequently fuse together and form a compound

nucleus with a mass smaller than the mass of the total initial system. This mechanism is called incomplete fusion.¹ At high bombarding energies it is very difficult to separate complete and incomplete fusion. Usually a measurement of both contributions is performed.

It should also be noted that fusion does not necessarily mean compound nucleus formation. In some cases the angular momentum of the fused nucleus is larger than the value for which the fission barrier of the compound nucleus vanishes. In this case we do not form a compound nucleus but a kind of equilibrated two center system which will fission in two fragments. Such a process has been called fast fission.² It also contributes to the fusion cross section because the mass distribution of the fast fission products is similar to the one of the fission following compound nucleus formation. In this way one usually talk about fission like fragments as far as these fission and fast fission products are concerned.

Fast fission phenomenon can also occur if the angular momentum of the fused system is smaller than the value for which the fission barrier of the compound nucleus vanishes. The mechanism is then called quasifission.³ It happens for systems which should give a compound nucleus with a fissility parameter Z^2/A larger than ~ 40 . In this case the compound nucleus cannot be formed, even if it has a non vanishing fission barrier, because its saddle configuration is too compact to be reached by the two center composite system formed during the reaction which will, therefore, decay in two fission like fragments.

We can summarize the above situation by saying that the mechanisms contributing to the fusion cross section are : compound nucleus formation, incomplete fusion, fast fission and quasifission. Of course, for a given system we do not have necessarily the occurrence of the four preceding mechanisms at the same time. However the way the fusion cross section is experimentally defined, as the sum of the evaporation residues and of the fission like cross sections, has no ambiguity. The ambiguity only comes when we want to decompose this cross section in the contribution of different mechanisms.

Nevertheless it should be noted that it is not always very easy to measure the fusion cross section. Indeed for symmetric systems in the entrance channel it is hard to deduce a fission cross section because the symmetric mass distribution is spoiled by a contribution from completely energy relaxed deep inelastic products. Another problem also comes in the measurement of the evaporation residue cross section of very asymmetric systems at high bombarding energy. In this case the compound nucleus is very excited and can evaporate a lot of particles. Consequently the evaporation residues can be mixed with deep inelastic products having a mass close to the one of the target.

2. Experimental techniques for fusion cross sections measurements

We shall now very briefly quote some of the main different techniques which can be used to measure the fusion cross section.

The simplest way to get the fission cross section is to detect the fission fragments by means of a time of flight telescope located at a laboratory angle which corresponds to an emission angle, of the fragments in the center of mass system, close to 90° . The reason is that one usually assumes that the angular distribution of the fission fragments, in the center of mass system, is $K/\sin\theta$. Consequently in the 90° region the cross section is very flat and this makes easy to calculate the total fission cross section. The time of flight telescope can be for instance a carbon foil located close to the target associated to channel plates which will multiply the number of primary electrons created in the carbon foil when the fission fragment passes through it. This detector provides a start signal. The stop signal is usually given by a fission solid state detector located at the time of flight distance from the carbon foil. The solid state detector also delivers an energy signal. The fission fragments are usually well separated from the other contributions if we look at the energy versus time of flight two-dimensional spectrum.

Because the fission process is binary and, at low bombarding energy, corresponds to full linear momentum transfer, it is in most of the cases sufficient to

detect only one of the fragments. However, when very heavy targets are used, the quasi target nuclei, which result from a deep inelastic process, can undergo fission. Such a process is called sequential fission and these fission fragments usually spoil those coming from fission following complete fusion. They can be removed if we require the coincidence between the two fragments. This can be done using for instance a multiwire proportional parallel plate counter as the one developed in ref.⁵ and which provides a localization of the correlated fission fragment in two dimensions. In fig. 1 are shown for the $^{35}\text{Cl} + ^{238}\text{U}$ system at 320 MeV [ref.⁶] the localization spectra in a direction parallel to the reaction plane (fig. 1a) and perpendicular to it (fig. 1b). The out of plane correlation comes from the deexcitation of the fission fragments by particle evaporation. For the other correlation there is in addition to the previous effect another broadening coming from the energy and mass distributions of the fission fragments. By requiring the coincidence between the time of flight telescope and this detector we can remove most of the sequential fission products.

The measurement of the evaporation residue cross section is a little bit more involved since one has to move close to the beam axis. The evaporation residues are usually identified by time of flight, or E- Δ E, or time of flight-E- Δ E telescopes. To get the total evaporation residue cross section it is needed to measure their angular distribution. The main experimental problem which arise in this kind of experiment is the relative normalization between the different angles, as well as the absolute normalization with the elastic scattering in order to get σ_{ER} . This necessitates a very good knowledge and stability of the beam axis, and also a very good beam quality. Such a measurement can nevertheless be simplified and the period of beam time be shortened if one measures several angles at the same time. This can be done for instance using a large area E- Δ E position sensitive ionization chamber as the one developed by Sann et al.⁷ In this case we can cover 22° in the reaction plane and as a consequence, in most of the cases, get the whole angular distribution of the evaporation residues at the same time. Such a set up has been used for instance to measure the $^{40}\text{Ca} + ^{40}\text{Ca}$ evaporation residues excitation function.⁹

3. First analysis of the fusion cross section

Very often the results concerning the fusion cross section are presented in terms of the critical angular momentum for fusion l_{CR} . This quantity is obtained from the experimental fusion cross section in a very simple and natural way which is nevertheless based on a few assumptions. The fusion cross section can be written in the following way :

$$\sigma_F = \frac{\pi}{k^2} \sum_{l=0}^{\infty} (2l+1) T_l \quad (2)$$

where k is the wave number :

$$k = \frac{\sqrt{2\mu E_{CM}}}{\hbar} \quad (3)$$

(μ the reduced mass and E_{CM} the center of mass energy) and T_l the transmission coefficient in the fusion channel for the l wave. It is usually assumed that it is the lowest l values which contribute to fusion. Furthermore, because the reduced wave length ($\lambda = 1/k$) of the system is small compared to the dimension of the nuclei, the T_l will go very rapidly to zero, in a range which is small compared to the number of l values contributing to the fusion process. This means that the sharp cut off approximation where one assumes that T_l goes from unity to zero is not too bad. Consequently we can rewrite σ_F as :

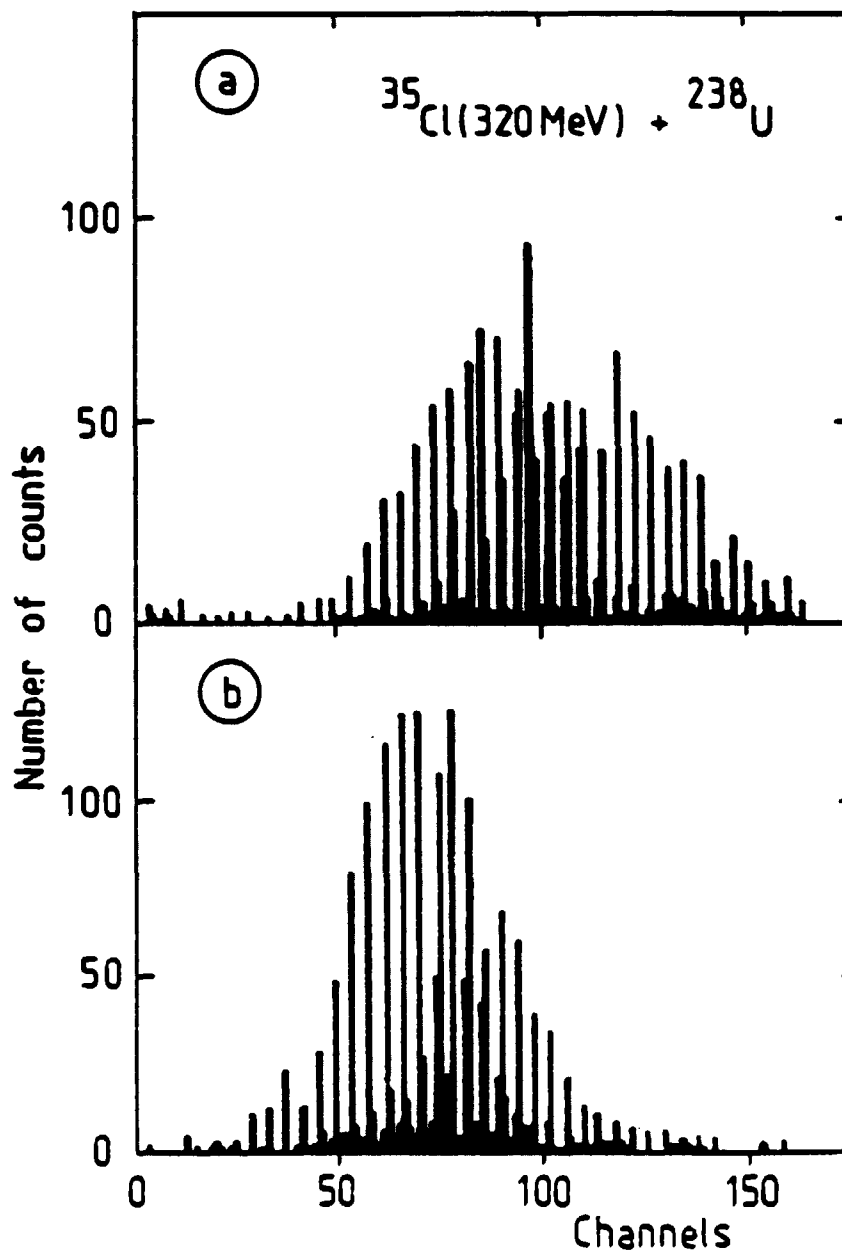


Fig. 1 - Spectra obtained with the multiwire proportional parallel plate counter of ref.⁵ in coincidence with a solid state detector (see text). a : in directions parallel to the reaction plane ; b : perpendicularly to it. These data have been taken on the 320 MeV Cl + U system investigated in ref.⁶.

$$\sigma_F = \frac{\pi}{k^2} \sum_{l=0}^{l_{CR}} (2l+1) = \frac{\pi}{k^2} (l_{CR}+1)^2. \quad (4)$$

In this way we have defined the critical angular momentum which is the largest l value leading to fusion.

It is interesting to parametrize the fusion cross section in terms of the critical angular momentum and look at its dependence upon the initial conditions of the reaction. The first important parameter on which depends l_{CR} is the bombarding energy : it increases as the bombarding energy increases. Furthermore, Zebelman and Miller⁹ have shown by forming the same compound nucleus, with different sets of projectiles and targets, that l_{CR} is a property of the entrance channel and not of the compound nucleus.

The evolution of the fusion cross section, for a given system, as a function of the bombarding energy exhibits three types of behaviour, depending on the energy range (see fig. 2) :

- In region 1, just above the fission threshold, the fusion cross section is linear as a function of the inverse of the center of mass energy. This is illustrated in fig. 3 for the Ni + ³⁵Cl systems.¹⁰ Close to the fusion threshold there are deviations from a straight line which can be explained in terms of quantum penetration of the fusion barrier.

- In region 2, σ_F is also linear as a function of the $1/E_{CM}$ but the slope has changed. In some cases, as it is illustrated in fig. 4 for the ¹⁶O + ²⁷Al system [ref.¹¹], the slope can even be positive. Therefore in region 2 there is a reduction of the fusion cross section compared to what would be expected by the extrapolation of region 1.

- Very few investigations have been done in the third regime but it seems that there is a dramatic decrease of the fusion cross section due to a saturation of the critical angular momentum. Furthermore, at these high bombarding energies, the fusion cross section is very likely spoiled by incomplete fusion. Fig. 5 illustrates on the ²⁴Mg + ⁶³Cu system¹² the possible existence of this regime.

The other piece of information which is very important is that heavy systems do not fuse anymore and this occurs when the product $Z_1 Z_2$ of the two atomic numbers of the projectile and of the target is larger than about 2500-3000.

4. Static interpretation of the fusion process

The aim is to understand, in the simplest way, the experimental results and if possible to predict fusion cross sections. Static models are very helpful in that respect. They are based on the fact that k is small compared to the dimensions of the system. This means that the two incident heavy ions will move on classical trajectories. Consequently the collision will be governed by the interaction potential between the two nuclei and we need to know this quantity for any interpretation.

The interaction potential between two heavy ions is usually calculated in the sudden approximation which assumes that the density of the two nuclei remain frozen during the collision. Such an approximation is a good one if the overlap between the two nuclei is not too large. This turns out to be the case for the configuration where the fusion process is decided. This is not too surprising since we have seen above that the fusion cross section mainly depend upon the entrance channel. The energy of the system corresponding to a superposition of the nuclear densities of the two ions can be calculated using for instance the energy density formalism¹³ which appears to be quite powerful and simple for such a calculation. In this formalism the energy density of a nuclear system, $\epsilon(\vec{r})$ can be written as a functional of the one body densities :

$$\epsilon(\vec{r}) = \epsilon [\rho_n(\vec{r}), \rho_p(\vec{r}), \rho_c(\vec{r})] \quad (5)$$

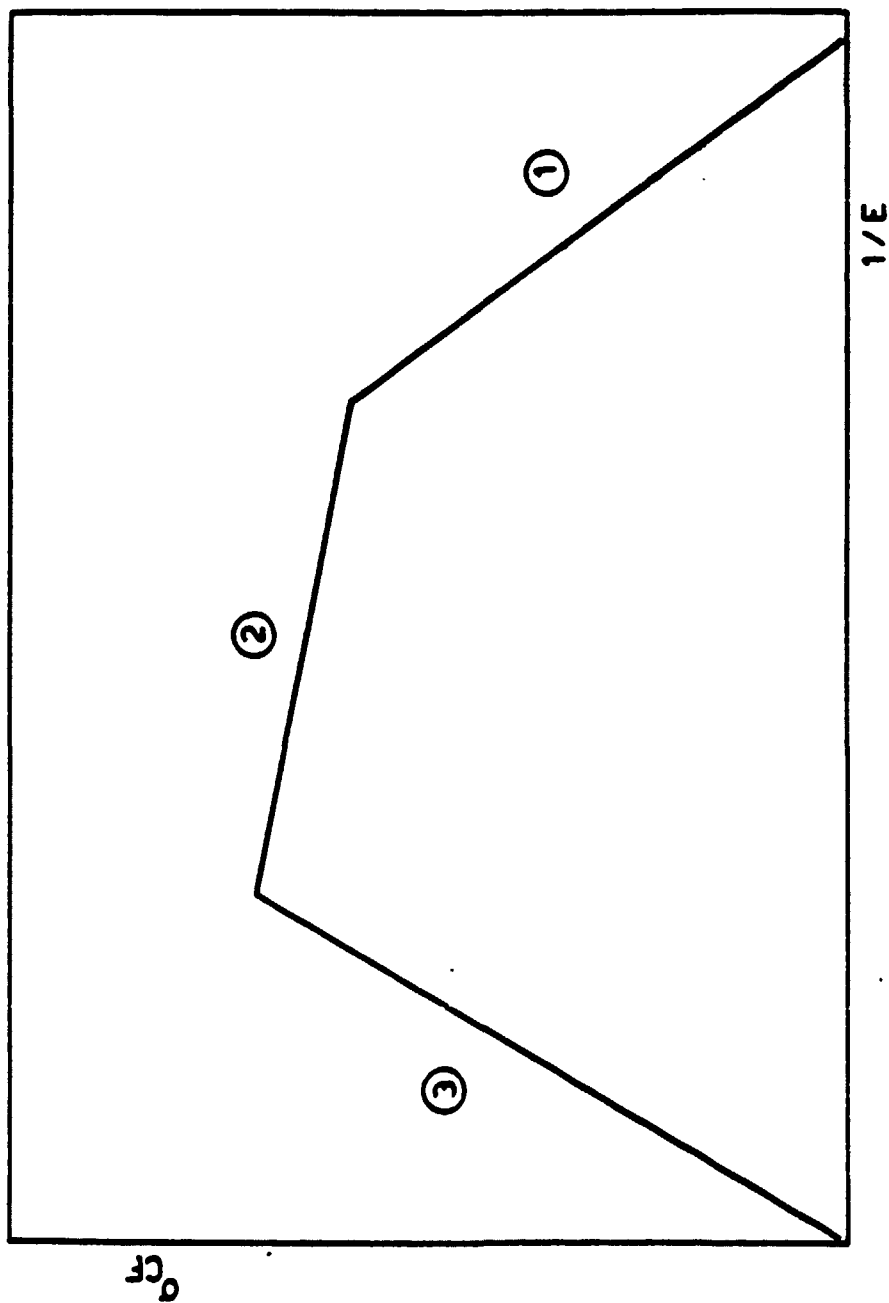


Fig. 2 - Schematic representation of the 3 regimes observed in fusion studies. σ_{CF} is the fusion cross section and E the center of mass energy.

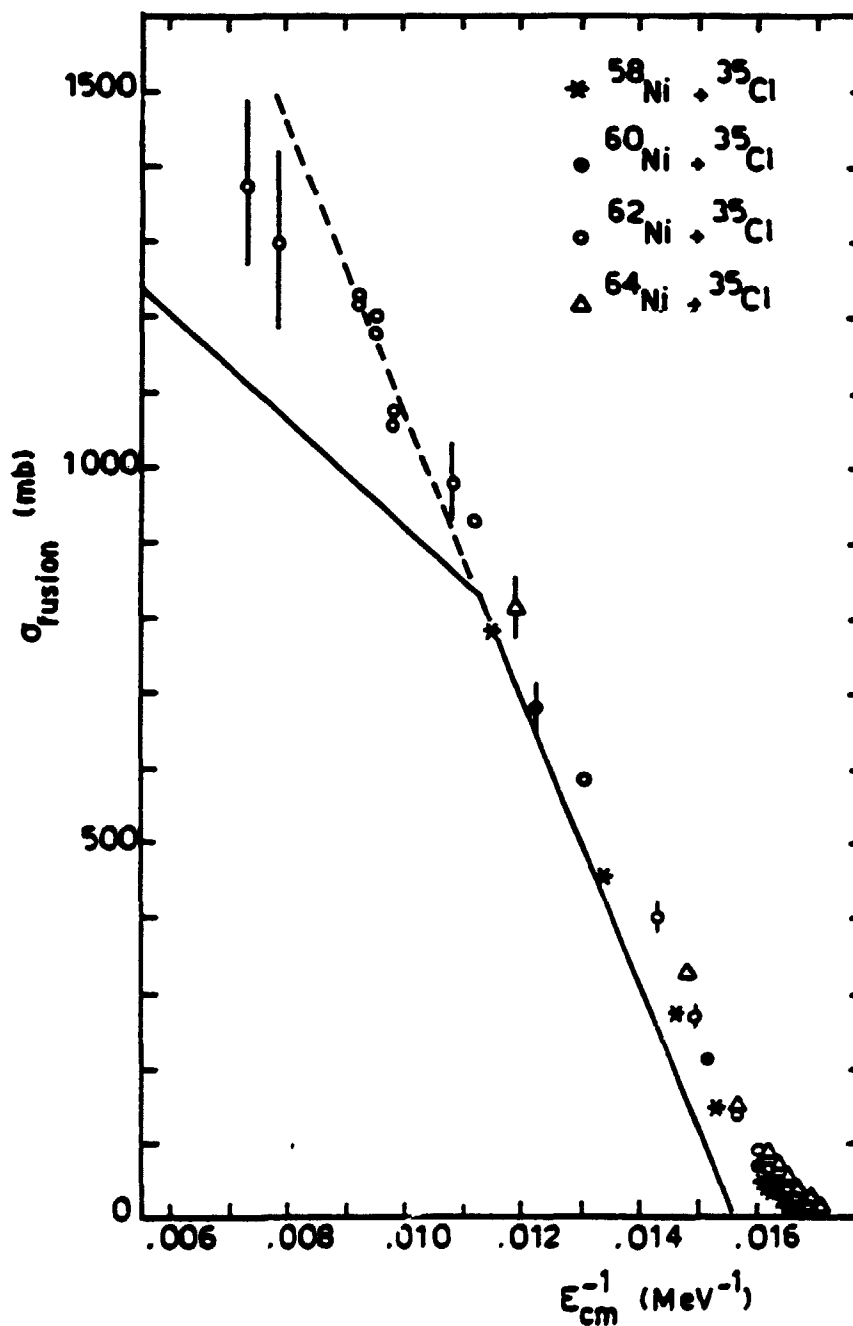


Fig. 3 - Fusion cross section versus the inverse of the center of mass bombarding energy. The experimental points are from ref.¹⁰. The full and the dashed curves are calculations done using the energy density potential of ref.¹³.

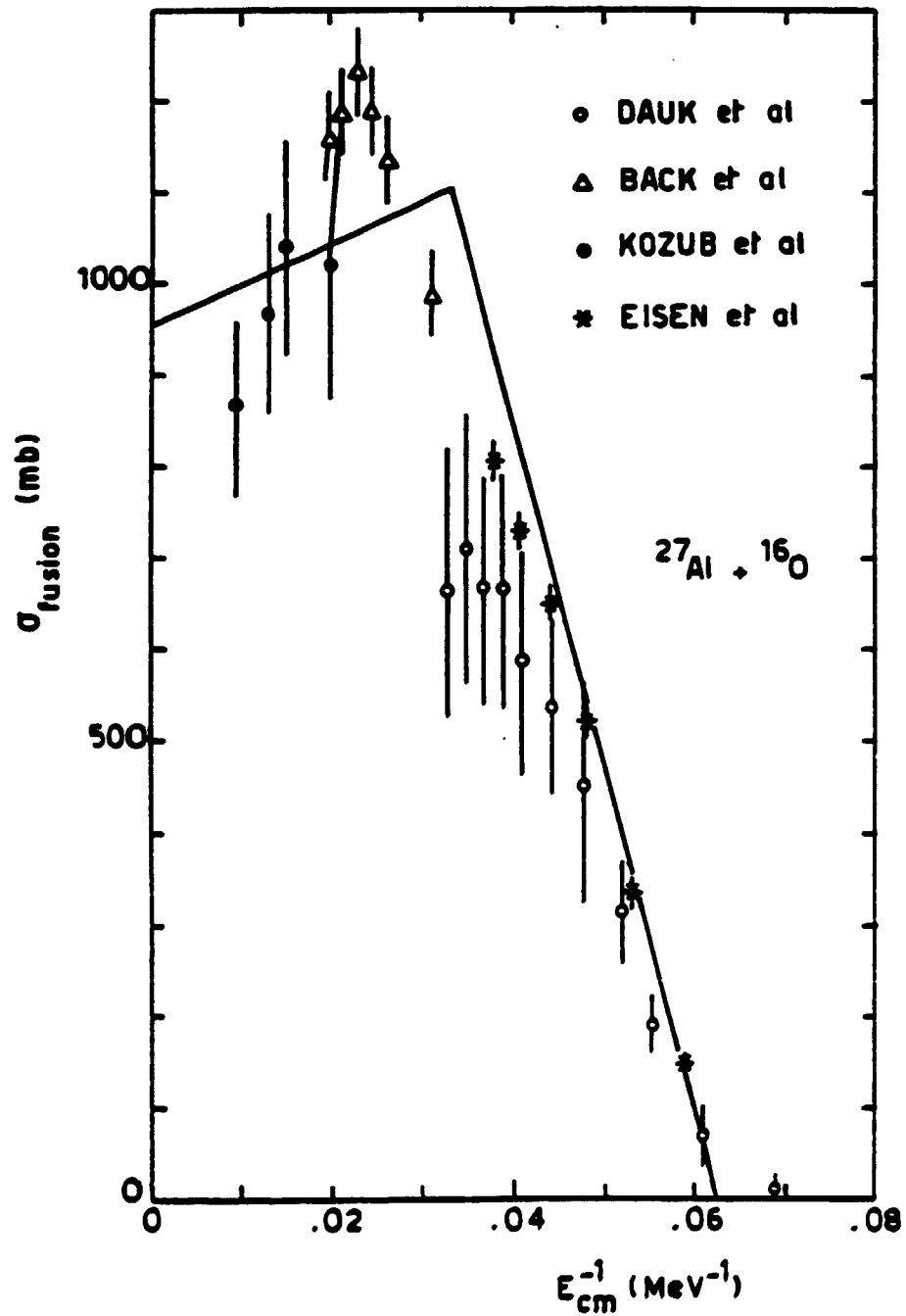


Fig. 4 - Same as fig. 3 for the $^{27}\text{Al} + ^{16}\text{O}$ system. The experimental points are from ref. 11.

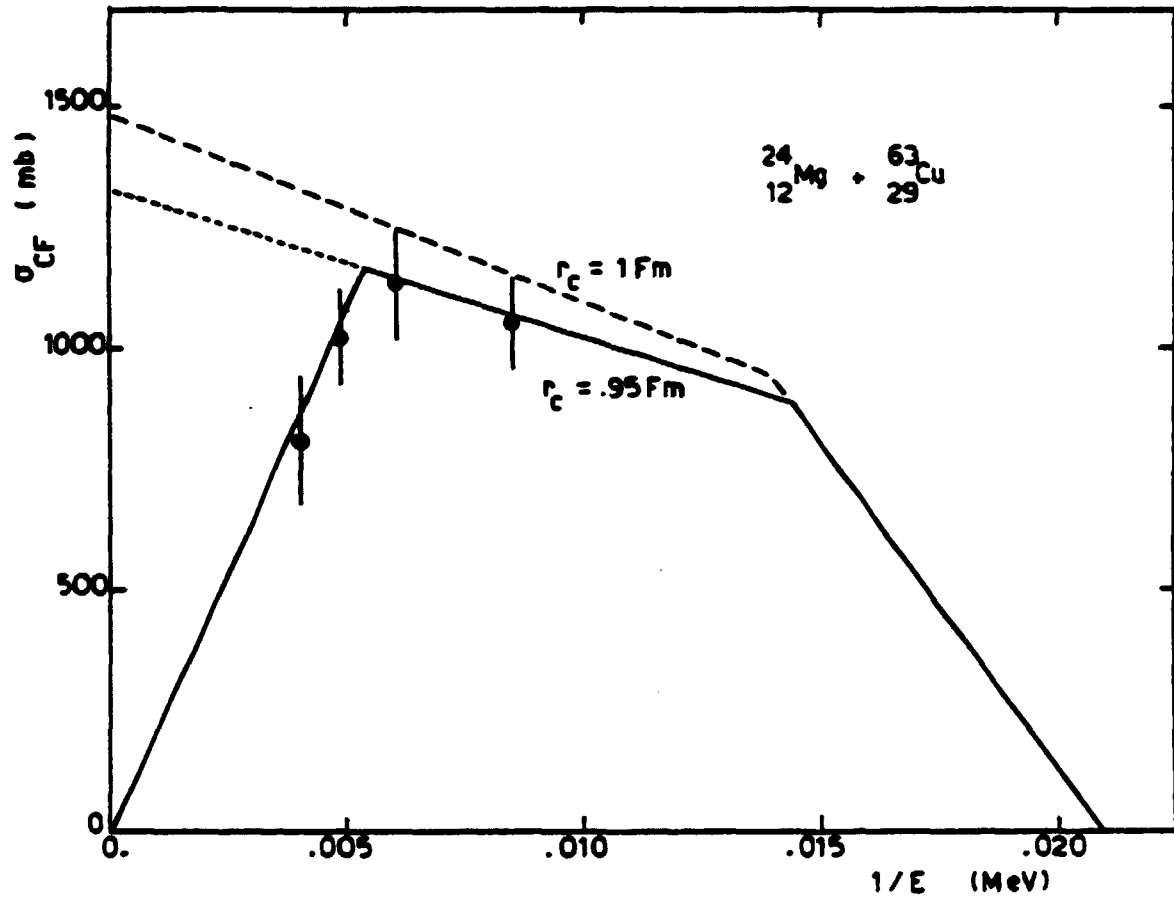


Fig. 5 - Same as fig. 4. From ref.¹².

where ρ_n , ρ_p and ρ_c are respectively the neutron, proton and charge densities. The total energy \mathcal{E} of the nuclear system is obtained by integrating this energy density over the whole space :

$$\mathcal{E} = \int \epsilon(\vec{r}) d\vec{r} \quad (6)$$

The inputs which are necessary to calculate \mathcal{E} are the analytic expression of the functional (which is not unique) and the parameters entering in its expression. These parameters are usually determined from the properties of infinite nuclear matter and from the binding energy of a given nucleus. The densities which are used in the calculation can be either generated by minimization or taken from other calculations. In the case of the sudden approximation, the interaction potential $V(R)$, is expressed as :

$$V(R) = \int \{ \epsilon(\rho_1 + \rho_2) - \epsilon(\rho_1) - \epsilon(\rho_2) \} d\vec{r}$$

where ρ_1 and ρ_2 stand for the set of densities of the projectile and of the target. R is the distance separating the center of mass of the two nuclei.

The total interaction potential $V(R)$ can be decomposed into two parts, a nuclear part $V_N(R)$, and a Coulomb part $V_C(R)$:

$$V(R) = V_N(R) + V_C(R) . \quad (7)$$

In fig. 6 are shown the nuclear, Coulomb and total interaction, potentials as a function of R for the Ar + Au system and for a head-on collision¹⁴. We observe that $V(R)$ exhibits a barrier, which is called fusion barrier, around 11 fm. It also exhibits a pocket located around 9 fm.

Static models usually assume that the 2 ions should come close enough to each other in order to fuse. The first guess is that they should overcome the fusion barrier. Then the overlap will be sufficient so that the system could be trapped, by friction forces for instance, into the pocket of $V(R)$. In fact the two heavy ions are shot on each other with different values of the impact parameter i.e. with different value of the orbital angular momentum λ . The total interaction potential including the centrifugal energy, $V_\lambda(R)$, is given by :

$$V_\lambda(R) = V(R) + \frac{\lambda(\lambda+1)\hbar^2}{2\mu R^2} . \quad (8)$$

Such an effective potential will, in many cases, have a barrier $V_\lambda(R_I(\lambda))$ located at $R_I(\lambda)$. If it is necessary for the system to overcome the fusion barrier the critical angular momentum will be given by the following expression :

$$E_{CM} = V_\lambda(R_I(\lambda_{CR})) \quad (9)$$

which expresses the fact that the center of mass energy is equal to the height of the barrier (no kinetic energy at this point). Eq.(9) can be rewritten as :

$$\lambda_{CR}(\lambda_{CR} + 1) = \frac{2\mu R_I^2(\lambda_{CR})}{\hbar^2} \{ E_{CM} - V(R_I(\lambda_{CR})) \} \quad (10)$$

assuming that

$$R_I(\lambda) \approx R_I(0) = R_I \quad (11)$$

and

$$\lambda_{CR}(\lambda_{CR} + 1) \approx (\lambda_{CR} + 1)^2 \quad (12)$$

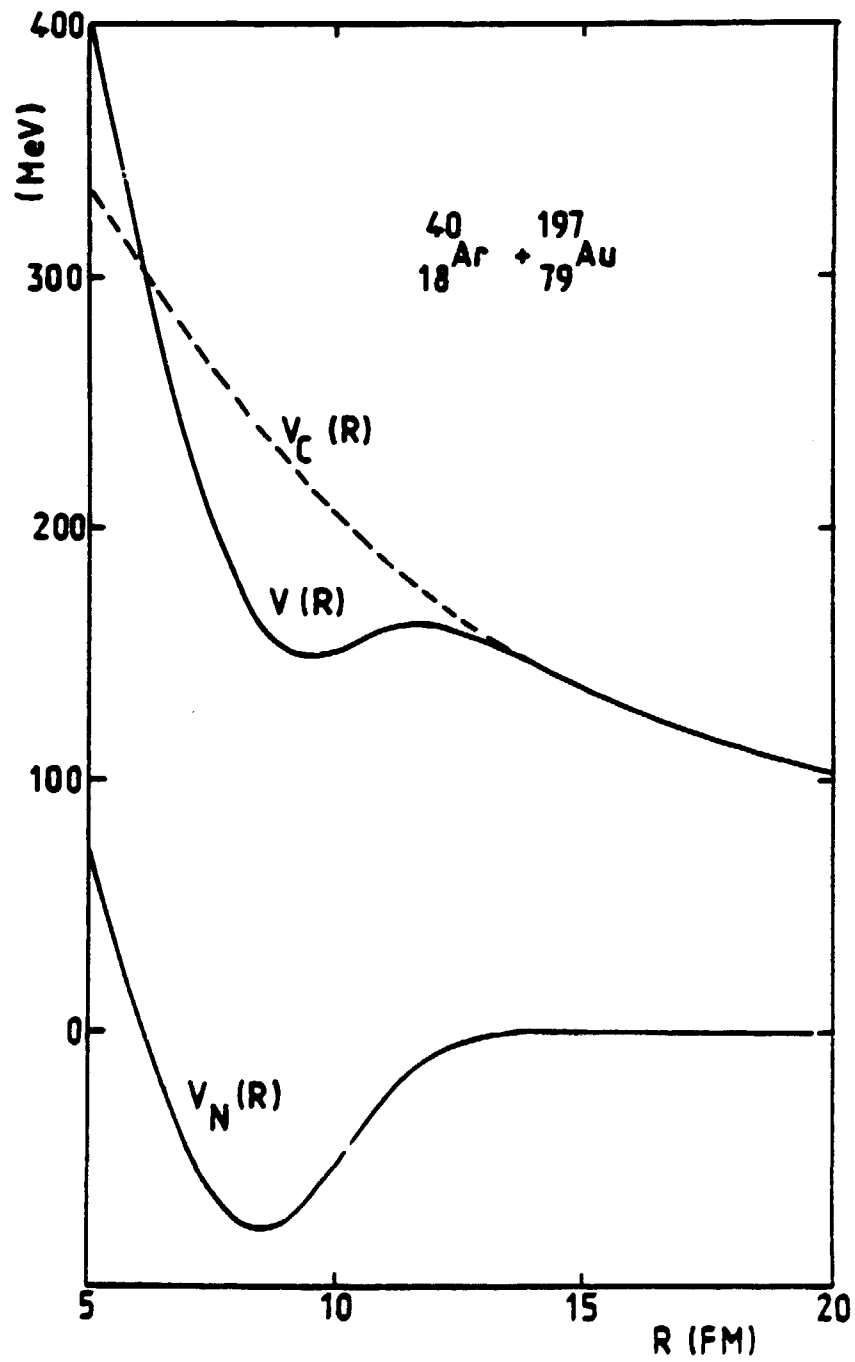


Fig. 6 - Total interaction potential $V(R)$ versus R . V_N is the nuclear part and V_C the Coulomb one. From ref.^{2,3}.

we can deduce that :

$$\sigma_F = \pi R_I^2 \left(1 - \frac{V_{12}}{E_{CM}} \right) \quad (13)$$

where $V_{12} = V(R_I(0))$ is the fusion barrier for a head on collision. Eq.(13) shows that the fusion cross section is linear as a function of $1/E_{CM}$ as it is observed experimentally. From the experiment we can therefore deduce V_{12} and R_I .

The above considerations would only predict one regime in the fusion cross section as a function of $1/E_{CM}$. This regime turns out to be the first one. However, as the bombarding energy increases, we are very often faced with a new regime where the fusion cross section is smaller than the one extrapolated from low energies using eq.(8). Because in the new regime σ_F looks also linear as a function of $1/E_{CM}$, it is tempting to parametrize the fusion cross section by an expression similar to eq.(13) :

$$\sigma_F = \pi R_C^2 \left(1 - \frac{V_C}{E_{CM}} \right) \quad (14)$$

where R_C is now a new distance called critical distance and $V_C = V(R_C)$. From the critical distance it is possible to deduce a critical radius parameter r_C :

$$r_C = \frac{R_C}{A_1^{1/3} + A_2^{1/3}} \quad (15)$$

Now the physical interpretation is the following and has been proposed by Galin et al.¹⁴ In the second fusion regime it is necessary for the system to reach a critical distance. But the nice thing in this idea is that the radius parameter r_C turns out to be almost constant for all systems ($r_C \approx 1$ fm). From the experimental data it is easy to deduce R_C and V_C and this also provides our knowledge of interaction potentials with a useful information.

The reason why there is a transition between the two regimes comes from the fact that for small λ values $V_C < V_{12}$. Consequently to reach R_C it is first necessary to overcome the fusion barrier. However when λ increases, due to the centrifugal energy which increases much more at R_C than at $R_I(\lambda)$, the effective critical potential $V_C + \lambda(\lambda+1)\hbar^2/(2\mu R_C^2)$ becomes larger than $V_2(R_I(\lambda))$. Consequently to reach the critical distance it is not sufficient to overcome the effective fusion barrier : one should give an extra energy. As a consequence σ_F is smaller. The above considerations concerning the two regimes have been presented by Glas and Mosel.¹⁵ Despite the success of the notion of critical distance, which is very useful for parametrizing the experimental data, there is still no real theoretical foundation of this notion. Furthermore the concept of critical distance, with a constant value of r_C , cannot explain the two following experimental facts : 1) that very heavy systems do not fuse ; 2) that there exist a third regime.

At this step it is necessary to introduce another condition for a system to fuse : we need that the total interaction potential for a given partial wave present a pocket to trap the system. If it is so, the system has time to reorganize and to reach a fused configuration. Otherwise it reseparates immediately. The system is trapped into the pocket due to friction forces which will act as soon as it reaches the interaction region. Of course such friction forces are not described by the static model. If we apply this necessary condition to the energy density potential we find that indeed, very heavy systems characterized by $Z_1 Z_2 > 2500-3000$ cannot fuse because the pocket has disappeared even for a head-on collision.

Such a condition also explains the existence of a third regime at high bombarding energy. Indeed the pocket can disappear because of angular momentum. Therefore when the bombarding energy is very high, large values of λ are involved and the system cannot be trapped anymore because of the disappearance of the pocket due

to angular momentum. This will lead to a limiting value of the critical angular momentum. It should be noted that the value of l where $V_2(R)$ does not present anymore a pocket is not the same as the limiting value of the critical angular momentum. Indeed, because of tangential friction, some orbital angular momentum is lost and, in the course of the collision, the system will feel a different potential $V_2(R)$. If we call l_{lim} this limiting value, we will have :

$$\sigma_F = \frac{\pi}{k^2} l_{lim}^2 . \quad (16)$$

This expression, which will describe the third regime, shows that σ_F decreases linearly as E_{cm} increases. However in this interpretation there is still an unknown, namely the amount of orbital angular momentum lost at the beginning of the reaction. An alternative explanation to the preceding one consists in saying that the compound nucleus becomes instable with respect to rotation when the angular momentum it carries, is larger than l_{Bf} , the value for which its fission barrier vanishes. Consequently we would expect that the critical angular momentum is bounded by l_{Bf} . However, for medium systems it has been shown that l_{CR} can be larger than l_{Bf} which means that fusion is not necessarily compound nucleus formation.²

Another kind of static models have been developed in order to explain σ_F . They are not based on entrance channel effects but, on the contrary, assume that the limitations for fusion are due to compound nucleus properties and more precisely on yrast line limitations.¹⁶ They have been mostly applied to light systems sometimes with some success. We will not describe them but refer the reader to ref.¹⁷ for more details.

Now we can come back to the experimental results presented in figs. 3-5 and see to which extent they can be reproduced by the energy density potential of ref.¹³

In fig. 3 the full line at small bombarding energies (large values of $1/E_{cm}$) is calculated by eq.(13). It rather well fits the experimental data except in the region close to the barrier where we observe a deviation due to quantum penetration which is not taken into account in eq.(13). This line is extrapolated by the dashed line which should not apply if the critical distance would work in this region because, then, we would get the second full line for large values of E_{cm} . Nevertheless we see that the experimental data are not reproduced in this case if we use the concept of critical distance and that they are better reproduced by eq.(13).

In fig. 4 we clearly see the need of using the critical distance concept to describe the second regime which is here quite apparent. A reasonable description is obtained although the excitation function is not reproduced in details.

In fig. 5 we show the calculation for the Mg + Cu system. As far as the critical regime is concerned, two values of r_c have been chosen : 0.1 and 0.95 fm. The latter value seems to better fit the experimental data. At high bombarding energy we see a deviation from the critical distance regime and this part is better described if we look at the disappearance of the pocket of $V(R)$ due to angular momentum and assuming that the sticking limit is reached.

Finally we show in fig. 7 the experimental data of ref.^{8,18} for the Ca + Ca system together with a calculation using the energy density potential and taking into account barrier transparency by means of the Hill and Wheeler formula.¹⁹ For this system we are in the first regime and we get a good fit of the data. It should be noted that the energy density potential works better for nuclei with a mass larger than $\sim 20-30$ because it is basically equivalent to a leptodermous approximation which does not work well for light nuclei. This can be clearly seen in fig. 8 where the error in percent between the calculated and the experimental fusion barriers are plotted against $Z_1 Z_2$ for different systems. This comparison was done in ref.²⁰ using the energy density potential of ref.¹³. For medium systems we see that there is a tendency to overestimate the fusion barrier by about 2 %. Systems characterized by $Z_1 Z_2 \leq 100$ are too light for applying this potential but nevertheless the error is in many cases smaller than 6 %.

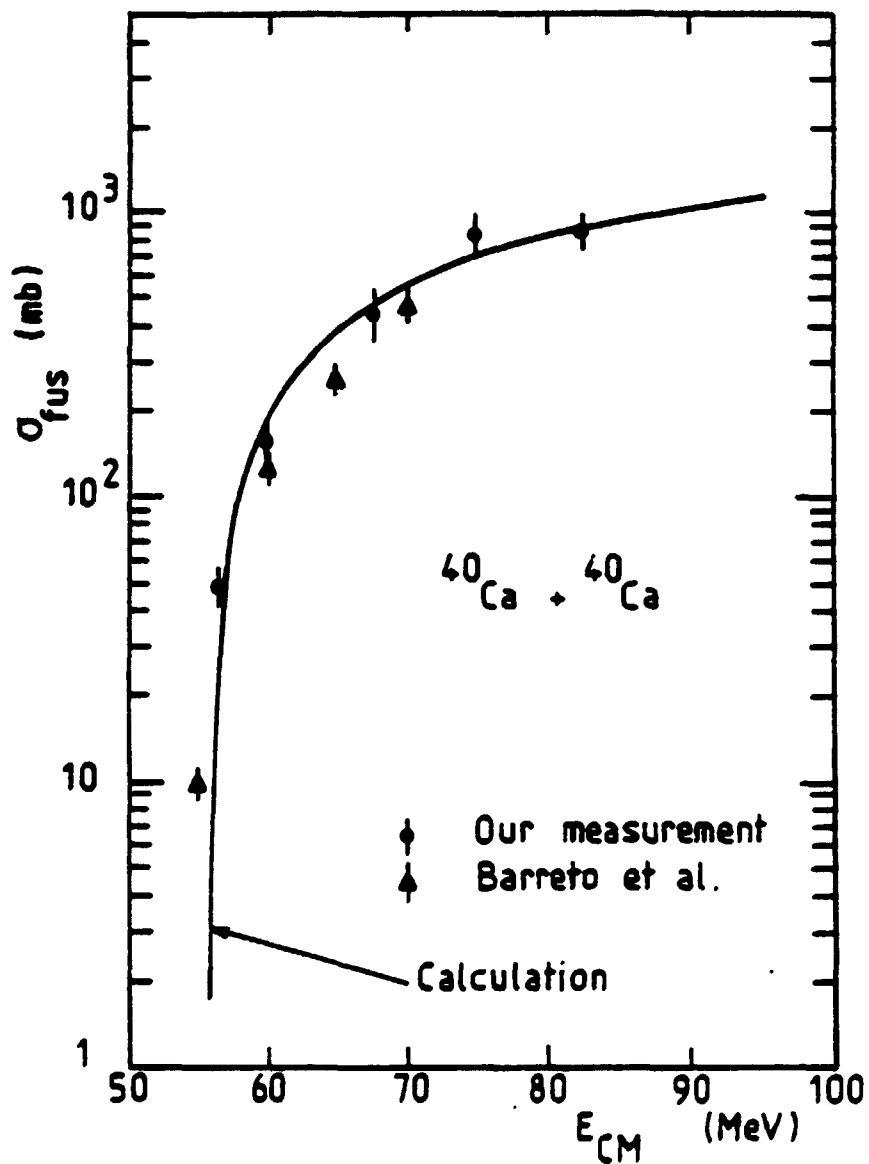


Fig. 7 - Fusion excitation function of the $^{40}\text{Ca} + ^{40}\text{Ca}$ system. The data are from ref.³ and¹⁸. The calculation from ref.³.

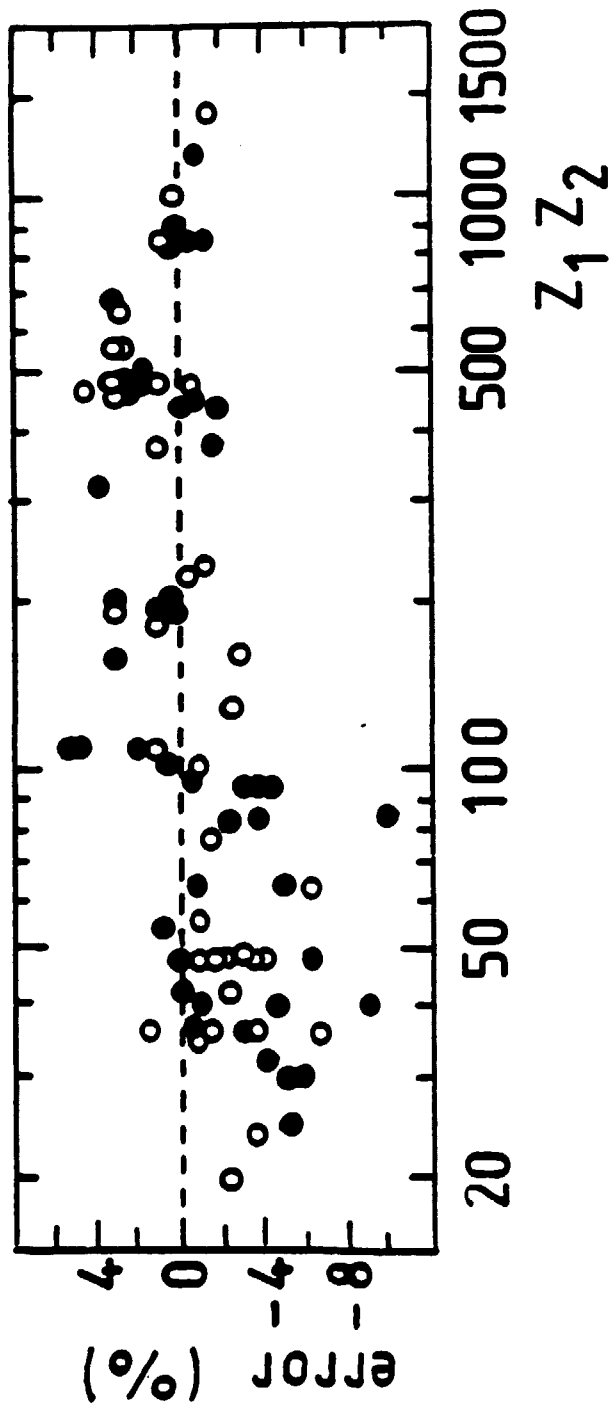


Fig. 8 - Error between calculated and experimental fusion barriers as a function of $Z_1 Z_2$ for different systems. Extracted from ref.²⁰ where the energy density potential of ref.¹ has been used.

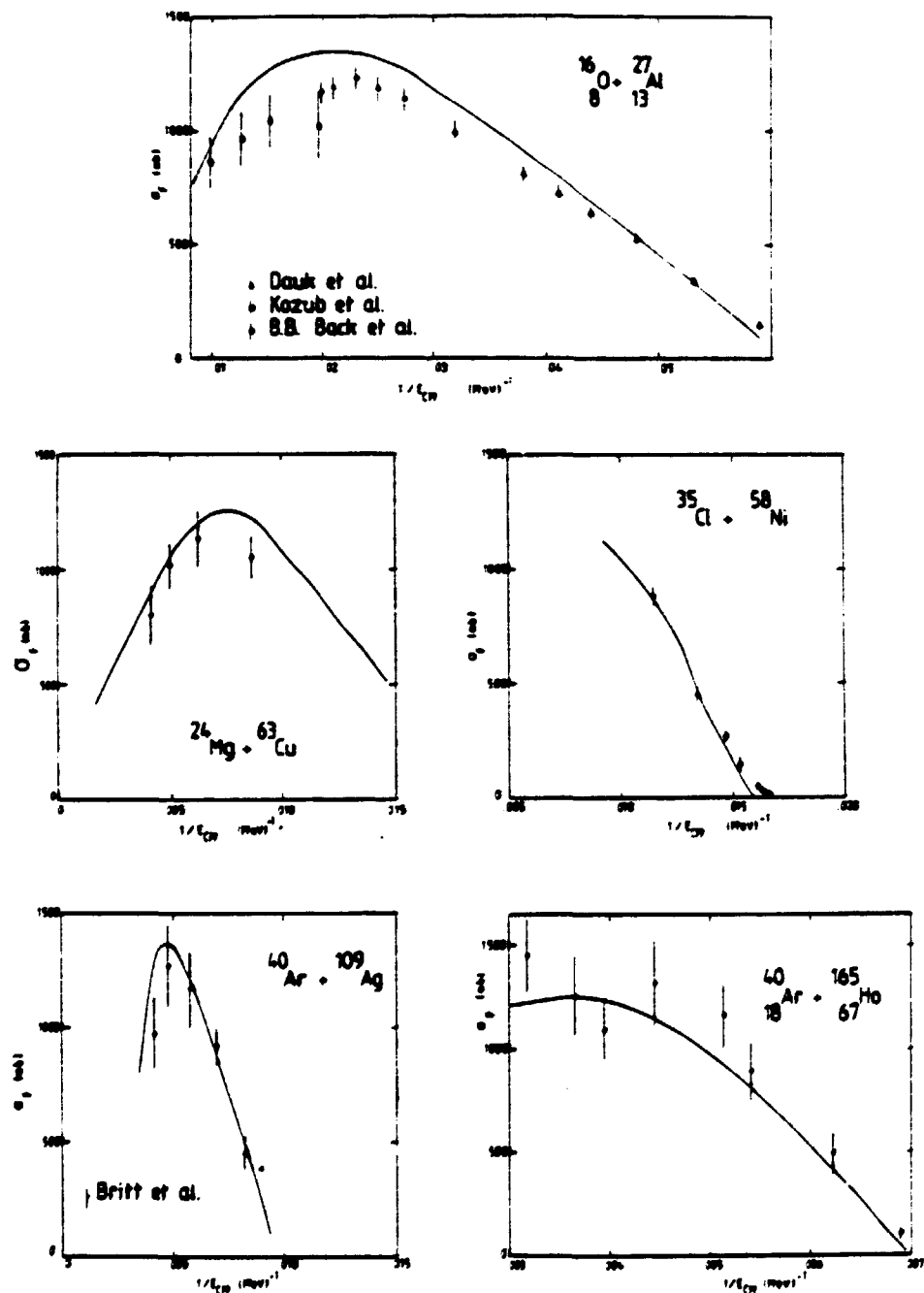


Fig. 9 - Excitation function for the $^{16}\text{O} + ^{27}\text{Al}$, $^{24}\text{Mg} + ^{63}\text{Cu}$, $^{35}\text{Cl} + ^{58}\text{Ni}$, $^{40}\text{Ar} + ^{109}\text{Ag}$, $^{40}\text{Ar} + ^{165}\text{Ho}$. The full curve is the result of the dynamical calculation of ref. 2). The experimental data are from ref. 9, 10, 11, 13, 25 and 27

5. Dynamical interpretation of the fusion process

Heavy ion reactions where a large number of nucleons are involved, like fusion or deep inelastic reactions, can be described in terms of a few macroscopic degrees of freedom which are of collective nature. These degrees of freedom are coupled to the remaining ones, the intrinsic degrees, which have a fast relaxation to equilibrium. This means that, as far as we only consider the macroscopic degrees, there is dissipation. A dynamical description of the collision can be done in terms of classical equations of motion (Newton equations) with friction forces.²¹ More involved approaches even include the fluctuations around the classical trajectories.²² In these dynamical approaches, fusion corresponds to the case where the system can be trapped into the pocket of the interaction potential due to friction force. The simplest model of this type, proposed by Gross and Kalinowski²¹ describes the collision with only two macroscopic variables R and θ , the radial distance and the polar angle. This model was quite successful in reproducing many fusion cross sections. Systematic calculations along this line have been performed in many systems and a reasonable agreement was obtained. In fig. 9 is shown the result of a calculation which we have performed²³ with a rather involved dynamical model²⁴ for different systems. We observe that we have a rather good description of the data.

It should be noted that in dynamical calculations we only observe two regimes in the fusion excitation function although we get a reasonable agreement with the experimental data. The first regime, at low bombarding energies comes from the fact that the system has to overcome the fusion barrier (this is similar to the case of static models). However at higher bombarding energy the fusion limitation comes from the disappearance of the pocket in $V(R)$ due to angular momentum. Therefore there is no need to introduce the critical distance concept.

It should also be noted that dynamical and static models will give almost the same fusion cross section in the first regime provided we use the same interaction potential. This could appear to be surprising since in a dynamical calculation the system will lose energy before it reaches the fusion barrier due to friction forces. Therefore we would expect a smaller σ_F . In fact it also loses angular momentum and it turns out that if the radial friction coefficient is half the value of the tangential friction one, both effects compensate.²⁷ The energy loss in the radial motion is compensated by the loss of orbital angular momentum which leads to a decrease of the fusion barrier. This condition between radial and tangential friction is predicted by the one body dissipation.²⁵

The main advantage of dynamical models is that they also allow to calculate other properties than the fusion cross section. In particular, depending on their degree of sophistication, they are able to describe many deep inelastic properties. However if we are only interested in fusion data, static models do as a good job and sometimes even better than dynamical models which are more difficult to operate.

6. Conclusion

We have seen in this brief review that we are now at a stage where we have an overall understanding of the fusion process. We should nevertheless not be too much optimistic because we have also seen that the agreement between the models and the data is not always perfect. More systematic investigations of the fusion excitation function with high resolution detection set up are needed. The new Legnaro tandem accelerator appears in that respect very useful and, without any doubt, we will see very soon many fascinating results concerning this field.

I am grateful to the Legnaro National Laboratory for financial support. I would also like to thank Mrs F. Lepage and E. Thureau for the material preparation of this manuscript.

References

- 1) For a review on incomplete fusion see for instance : C. Gerschel, International Conference on selected aspects of heavy ion reactions, Saclay (1982) ; Nucl. Phys. A387 (1982) 297c.
- 2) For a review on fast fission : C. Ngô, C. Grégoire, B. Remaud and E. Tomasi, International conference on nucleus-nucleus collisions, Michigan (1982) ; Nucl. Phys. (1983) in press.
- 3) W.J. Swiatecki, Physica Scripta 24 (1981) 113 and Nucl. Phys. A376 (1982) 275.
- 4) P. Dyer, R.J. Puigh, R. Vandenbosch, T.D. Thomas and M.S. Zisman, Phys. Rev. Lett. 39 (1977) 392.
- 5) C. Mazur and M. Ribrag, Nucl. Instr. Meth. (1983) in press.
- 6) S. Leray, X.S. Chen, G.Y. Fan, C. Grégoire, H. Ho, C. Mazur, C. Ngô, A. Pfoh, M. Ribrag, L. Schad, E. Tomasi and J.P. Wurm, XXI Bormio Conference (1983).
- 7) H. Sann, H. Damjantschitsch, D. Hebbard, J. Junge, D. Pelte, B. Povh, S. Schwalm and D.B. Tran Thoai, Nucl. Instr. Meth. 124 (1975) 509.
- 8) E. Tomasi, D. Ardouin, J. Barreto, V. Bernard, B. Cauvin, C. Magnago, C. Mazur, C. Ngô, E. Piasecki and M. Ribrag, Nucl. Phys. A373 (1982) 341.
- 9) A.M. Zebelmann and J.M. Miller, Phys. Rev. Lett. 30 (1973) 27.
- 10) W. Scobel, H.H. Gutbrod, M. Blann and A. Mignerey, Phys. Rev. C14 (1976) 1808. P. David, J. Bisplinghoff, M. Blann, T. Mayer-Kuckak and A. Mignerey, Nucl. Phys. A287 (1977) 179.
- 11) J. Dauk, K.P. Liew and A.M. Kleinfeld, Nucl. Phys. A241 (1975) 170. B.B. Back, R.B. Betts, C. Gaarde, J.S. Larsen, E. Michelsen and Tsai Kuong-Hsi Nucl. Phys. A285 (1977) 317. R.L. Kozub, N.H. Lu, J.M. Miller, D. Logan, T.W. Debiak and L. Kowalski, Phys. Rev. C11 (1975) 1497. Y. Eisen, I. Tserruya, Y. Eyal, Z. Fraenkel and M. Hillman, Nucl. Phys. A241 (1977) 459.
- 12) B. Borderie, M. Berlinger, R. Bimbot, C. Cabot, D. Gardès, C. Grégoire, F. Hanappe, C. Ngô, L. Nowicki and B. Tamain, Z. Phys. A298 (1980) 235.
- 13) H. Ngô and C. Ngô, Nucl. Phys. A348 (1980) 140.
- 14) J. Galin, D. Guerreau, M. Lefort and X. Tarrago, Phys. Rev. C9 (1974) 1018. R. Bass, Nucl. Phys. A231 (1974) 45.
- 15) D. Glas and U. Mosel, Nucl. Phys. A237 (1975) 429.
- 16) S.M. Lee, T. Matsuse and A. Arima, Phys. Rev. Lett. 45 (1980) 165.
- 17) For a review see for instance U. Mosel, Dynamics of heavy ion collisions, 3rd Adriatic Study Conference on the dynamics of heavy ion collisions, Hvar (1981) edited by N. Lindero, R. Ricci and W. Greiner, North Holland, p.1.
- 18) J. Barreto, Thèse d'Etat, Orsay (1980).
- 19) D.L. Hill and J.A. Wheeler, Phys. Rev. 89 (1953) 1102.
- 20) L.C. Vaz and J.M. Alexander, preprint 1980.

- 21) D.H.E. Gross and H. Kalinowski, Phys. Lett. 48B (1974) 302.
- 22) H. Hofmann and P.J. Siemens, Nucl. Phys. A275 (1977) 464.
C. Ngô and H. Hofmann, Z. Phys. A282 (1977) 83 ; Phys. Lett. 65B (1976) 97.
- 23) E. Tomasi, C. Grégoire, C. Ngô and B. Remaud, J. Phys. Lett. 43 (1982) L115.
- 24) C. Grégoire, C. Ngô and B. Remaud, Phys. Lett. 99B (1981) 17 ; Nucl. Phys. A383 (1982) 392.
- 25) J. Blocki, J. Randrup, W.J. Swiatecki and C.F. Tsang, Ann. Phys. 105 (1977) 427.
- 26) C. Lebrun; F. Hanappe, J.F. Lecolley, F. Lefebvres, C. Ngô, J. Peter and B. Tamain, Nucl. Phys. A321 (1979) 207.
B. Borderie, J. Peter, B. Tamain, S. Agarwal, J. Girard, C. Grégoire, J. Matuszek and C. Ngô, Z. Phys. A299 (1981) 263.
- 27) H.C. Britt, B.H. Erkkila, R.G. Stokes, H.G. Gutbrod, F. Plasil, R.J. Ferguson and M. Blann, Phys. Rev. C13 (1976) 1483.

